Original Paper

Study of Implanted B^+ and P^+ Ions into Si (100) for Ultra Shallow Junction by SIMS

Youn-Seoung Lee, Won-Jun Lee*, Myeung Hee Lee**, and Sa-Kyun Rha***
Dep. of Information Communication Eng, Hanbat National University, Daejeon 305-719, Korea,
**Department of Advanced Materials Eng. Sejong University, Seoul 143-747, Korea*
*** Dep. of Physics, College of Liberal Arts and Science, Yonsei University, Wonju 220-840, Korea,*
****Department of Materials Science Eng, Hanbat National University, Daejeon 305-719, Korea*
skrha@hanbat.ac.kr

(Received: November 26, 2007; Accepted: January 25, 2008)

We investigated a behavior of boron and phosphorous by the variation of B^+ and P^+ ion implantation energy (0.5 keV, 1 keV, and 2 keV) and rapid annealing temperature (950 ºC, 1000 ºC, and 1050 ºC) for the dose 1 x 10^{15} atoms/cm^2. The B^+ and P^+ ions were implanted into n-type and p-type Si (100) which the native oxide layer was removed , respectively. In order to investigate the B^+ and P^+ ion behavior by ion implantation, the junction depth Xj, the retained dose and the sheet resistance R_s was measured by using SIMS and 4-point probe. By the results, the diffusion length ΔX_j for P^+ implanted samples was larger than that for B^+ implanted samples, the retained dose of ^{31}P increased while one of ^{11}B decreased with increasing the RTA temperature, the variation of sheet resistance R_s value in B^+ implanted samples was larger than that of P^+ implanted samples with variation RTA temperature, and the effective mobility by temperature variation was more enhanced than that by implantation energy. Finally, we found that higher temperature process is needed to minimize the amount of residual defects in the substrate and obtain higher effective mobility.

1. Introduction

As higher gate densities and higher frequencies are required for Si integrated circuits, the scaling down of MOS electronic device dimensions is required. By projected design rule, junction depth at channel as shallow as 10-20 nm will be needed by the year 2012 [1].

Ion implantation has become a major production process as a common method in the semiconductor industry. Therefore, low-energy ion implantation of sub-keV has been considered to be the most promising candidate for the formation of shallower junctions [2-10]. Recently, the implant species of greatest interest have been boron (B) as p-type dopant and phosphorous (P) as n-type dopant, respectively [11].

In the present study, in order to deeply understand the diffusion, activation and the dopant-defect interaction etc., we have performed a comparative study for B and P dopants with various rapid thermal annealing (RTA) temperatures and various ion implantation energies.

2. Experiments

Si wafers of (100) orientation were used as a substrate material. In order to obtain a clean Si surface, the native oxide layer on Si wafer was removed by a diluted HF dip.

The B^+ and P^+ ion implantations were performed on a Varian VIISta 80 implanter with various implantation energies (0.5 keV, 1 keV, 2 keV) and dose 1 x 10^{15} atoms/cm^2 into n-type and p-type Si wafers, respectively. In order to reduce transport due to channelling, Si (100) wafer was tilted by 7º. After the implantation, rapid thermal annealing (RTA200H-SP1 of New Young M Tech.) for the samples was performed under N_2 ambient (760 Torr) at 950 ºC, 1000 ºC and 1050 ºC for 10 s. In addition, after the removal of the native oxide layers for all the implanted samples formed during the heat treatment process by a BOE dip, B and P depth profiles and a sheet resistance were measured.

The concentration depth profiles of ^{11}B and ^{31}P have been obtained by secondary ion mass spectrometry (SIMS),

using a Cameca ImS-6f Magnetic Sector SIMS in Korea Basic Science Institute (KBSI). The 2 keV O_2^+ primary ion beam was used for profiling the boron and phosphorous. The sputtered area of the primary ion beam (raster size) was 250 μm x 250 μm. The junction depth was measured at ^{11}B and ^{31}P concentration of 10^{18} atoms/cm^3. The conversion of data collection time to depth was determined by measuring the SIMS craters with a Tencor P-2 stylus profilometer. The accuracy of the depth scales is in the ±5 % range, with a precision of 2 %. Quantification of the SIMS profiles was accomplished by analyzing a boron doped Si standard (KRISS CRM 03-04-300) and a Phosphorus implanted standard (CEA reference materials).

The sheet resistance was measured with a 4-point probe.

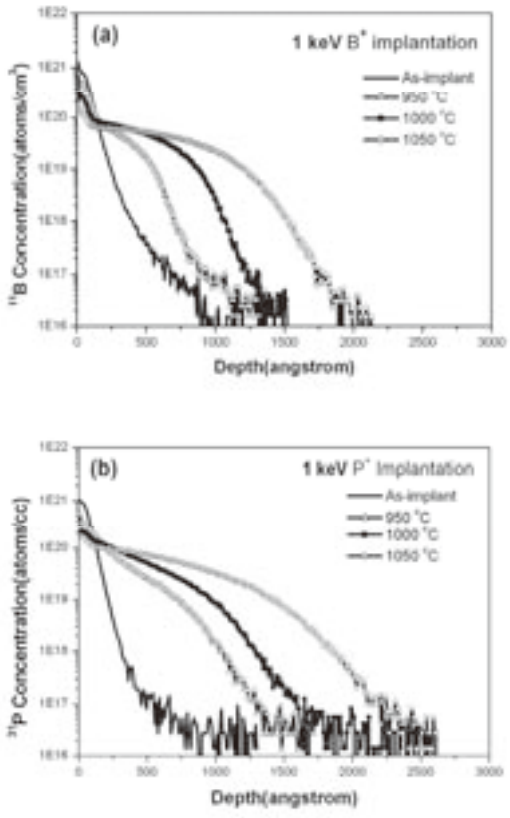

Figure 1. As-implanted and rapid thermal annealed SIMS profiles for 1 keV (a) boron B^+ and (b) phosphorous P^+ ion-implanted samples.

3. Results and discussion

Figs. 1(a) and 1(b) show the SIMS boron (^{11}B) and phosphorous (^{31}P) profiles, respectively. The SIMS profiles reveal bulk diffusion of boron and phosphorous into bulk Si.

Fig. 2(a) shows the junction depth (X_j) obtained from SIMS data of Fig. 1. Although the junctions for as-implanted samples are very shallow (below ~ 50 nm) for all samples, the junctions are deeper after RTA as shown in Fig. 2(a). Upon annealing, this result means an inter-diffusion of dopants.

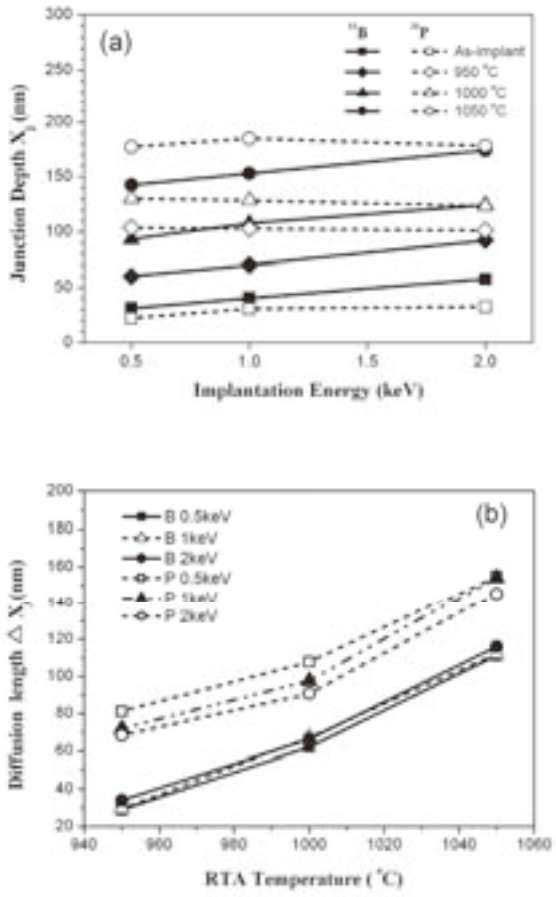

Figure 2. (a) Junction depth as a function of the B^+ and P^+ ion implantation energy and (b) diffusion length as a function of the RTA temperature: at $1x10^{18}$ atoms/cm^3 for as-implanted samples and for samples after RTA(950 °C ~1050 °C)

In case of B^+ implantation samples, the X_j increase linearly with increasing implantation energy and RTA temperature. However, the X_j for P^+ implantation samples hardly change with variation of implantation energy. In Fig. 2(a), at ≤1 keV the X_j of P^+ implanted samples is larger than that of B^+ implanted samples, but the X_j at 2 keV is similar nearly, except for all as-implanted samples.

The diffusion length ΔX_j is defined as the difference between the annealed and the as-implanted junction depths. On the whole, the diffusion length [Fig. 2(b)] increases with increasing RTA temperature. By compari-

son of B^+ with P^+ ion implantation, ΔX_j for P^+ implanted samples is larger than that for B^+ implanted samples. By this result, we can summarize he ΔX_j for P^+ implanted samples depends on both implantation energy and RTA temperature, but the ΔX_j for B^+ implanted samples depends on only RTA temperature and is independent of implantation energy.

Fig. 3 shows the ^{11}B and ^{31}P retained dose evaluated from SIMS data. In variation of ^{11}B retained dose, we can see the typical results; the retained dose increases with increasing the B^+ implantation energy and decreases with increasing the RTA temperature. Generally, in process of RTA, SiO_2 layer formed on Si wafer surface. As previous reports [10,12], the loss of the ^{11}B dose occurs because the SiO_2 layer leads to a out-diffusion of B dopant via surface evaporation. On the contrary, the retained dose of ^{31}P increases with increasing the RTA temperature. Recently, the similar effects with our studies was reported [11,13]: upon annealing, SiO_2 layer on Si surface leads to the segregation of ^{31}P and As dopants into the interface. Finally, we can obtain a conclusion that the ^{31}P retained dose increases

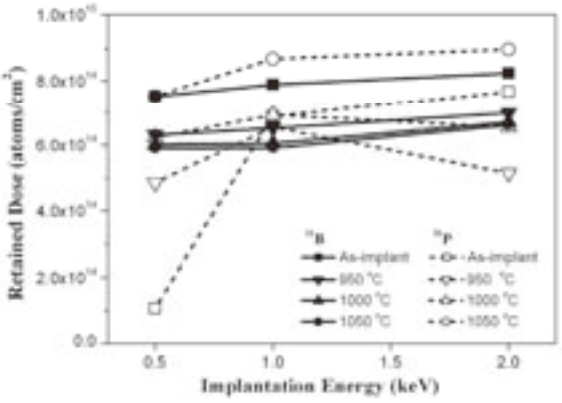

Figure 3. ^{11}B and ^{31}P retained dose by SIMS as a function of implantation energy for all samples (as-implanted and RTA treated samples)

with increasing the RTA temperature because SiO_2 layer formed in process of RTA plays a barrier role of ^{31}P out-diffusion. In case of B^+ implantation samples which the X_j increases linearly with increasing implantation energy and RTA temperature, the sheet resistance value R_s in Fig. 4 decreases with increasing implantation energy and RTA temperature. In addition, for P^+ implantation samples which the X_j hardly change with variation of implantation energy, the R_s is continuous nearly with increasing implantation energy. For the most part, the sheet resistance values R_s were lower with increasing RTA temperature. In a point of view that X_j is inverse proportion to R_s, that is, if X_j increases, R_s decreases [10], these results agree well with the expectation.

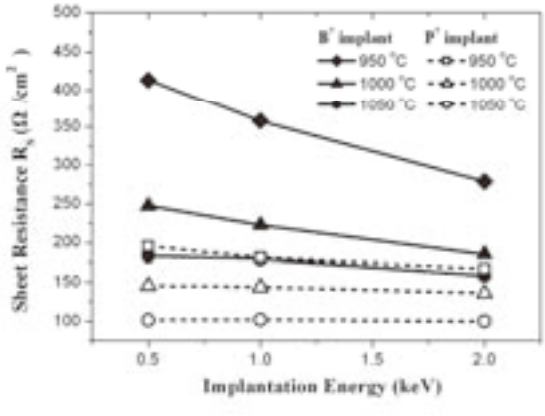

Figure 4. Sheet resistance(R_s) as a function of implantation energy for all samples (B^+ and P^+ as-implanted and RTA treated samples)

By comparison of B^+ with P^+ ion implantation, the variation of Rs value in B^+ implanted samples was larger than that of P^+ implanted samples with variation RTA temperature. In general, the implanted dopants in junction are electrically activated by RTA, and the active dopants can be lead to a decrease in R_s.

Induced defects by ion implantation will hinder the carrier transportation and lead to the degradation of mobility. The effective mobility μ in Fig. 5 was estimated by equations (1) and (2).

$$R_s = \frac{<\rho>}{X_j} = \frac{1}{X_j} \cdot \frac{1}{q \cdot \mu \cdot n} \quad \left(n = \frac{D}{X_j} \right) \quad (1)$$

where <ρ> and Xj are effective resistivity and thickness of the doped layer (=junction depth in SIMS result), respectively [14]. Therefore, the equation of effective mobility μ is as follows.

$$\mu = \frac{1}{q \cdot R_s \cdot D} \quad (2)$$

where R_s and D are sheet resistance in Fig. 4 and sheet carrier concentration (= retained dose in SIMS results) in Fig. 3, respectively. Charge q is 1.6 x 10^{-19} C. We assumed that these dopants (= retained dose) are completely ionized. By above equation, effective mobility μ

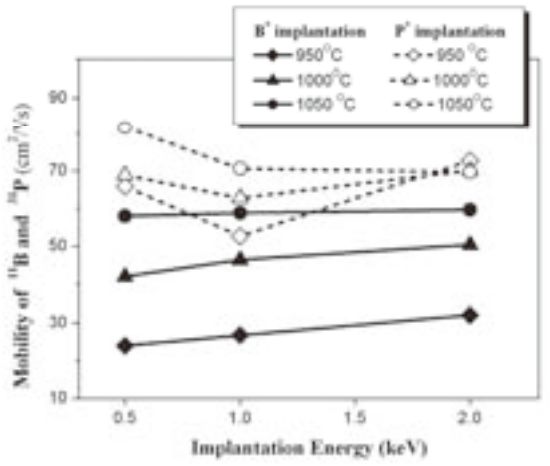

Figure 5. Effective mobility of ^{11}B and ^{31}P as a function of ion implantation energy for all samples. The values of effective mobility are estimated by measured R_s and retained dose.

should be inverse proportional to R_s and D.

In Fig. 5, the B^+ effective mobility small increased with increasing the implantation energy, especially, by variation of temperature was more enhanced than that by implantation energy. However, although the tendency in P^+ implanted samples was different from B^+ implanted samples, the increase of mobility by annealing was similar. In addition, for P^+ ion implanted samples, it seems that the μ value is independent with R_s. From these results, it was conclude that higher temperature process is needed to minimize the amount of residual defects in the substrate and obtain higher effective mobility.

4. Summary

We investigated a behavior of B and P by the variation of B^+ and P^+ ion implantation energy and RTA temperature. To summarize, the results are as follows.

In case of B^+ implantation samples, the junction depth X_j increased linearly and the sheet resistance value R_s decreased with increasing implantation energy and RTA temperature. However, the diffusion length ΔX_j depended on only RTA temperature and was independent of implantation energy. The retained dose ^{11}B increased with increasing the B^+ implantation energy and decreased with increasing the RTA temperature. Upon annealing, the loss of ^{11}B dose occurs due to out-diffusion of B dopant through the surface SiO_2 layer. The B^+ effective mobility by annealing was more enhanced than that by implantation energy.

In P^+ implantation samples, although the X_j hardly change with variation of implantation energy and increased by only annealing, the ΔX_j for P^+ implanted samples depends on both implantation energy and RTA temperature. In particular, the retained dose of ^{31}P increased while one of ^{11}B decreased with increasing the RTA temperature because of the segregation of ^{31}P into the SiO_2/Si interface. The R_s was continuous nearly with increasing implantation energy and was lower with increasing RTA temperature. In addition, it seemed that the P^+ effective mobility value is independent with R_s.

Acknowledgements

This work was supported by "System IC 2010" project of Korea Ministry of Commerce, Industry and Energy.

5. References

[1] International Technology Roadmap for Semiconductors, Semiconductor Industry Association (2001).
[2] V. Privitera, Current Opinion in Solid State and Materials Science 6, 55 (2002).
[3] H. –S. Park, K. Jeong, H.-W. Suh, H.-J. Jung, and W.-K. Choi, J. Korean Phys. Soc. 44(6), 1594 (2004).
[4] W. S. Yoo and K. Kang, Nucl. Instr. and Meth. in Phys. Res. B237, 12 (2005).
[5] C. Hongo, M. Tomita, M. Takenaka, and A. Murakoshi, Appl. Surf. Sci. 203-204, 264-267 (2003)
[6] J. Seo, O. Kwon, K. Kim, and T. Won, J. Korean Phys. Soc. 45, 1244 (2004).
[7] S. Ruffell, I.V.Mitchell, and P. J. Simpson, Nucl. Instr. and Meth. B242, 591 (2006).
[8] Junzo Ishikawa, J. Korean Phys. Soc. 48, 703 (2006)
[9] G. Mannino, S. Whelan, E. Schroer, V. Privitera, P. Leveque, G. G. Svensson, and E. Napolitani, J. Appl. Phys. 89, 5381 (2001).
[10] Woo-Jung Lee, Youn-Seoung Lee, Kwang-Su Cheong, Sa-Kyun Rha, Ki-Man Kim and Won-Jun Lee, J. Korean Phys. Soc. 50, 657 (2007).
[11] M. A. Bolorizadeh, S. Ruffell, I. V. Mitchell and R. Gwilliam, Nucl. Instr. and Meth. B225, 345 (2004).
[12] A Dusch, J. Marcon, K. Masmoudi, K. Ketata, F. Olivie, M. Benhzor, and M. Ketata, Nucl. Instrum Methods in Phys. Res. B186, 360 (2002).
[13] M. Tomita, M. Suzuki, T. Tachibe, S. Kozuka and A. Murakoshi, Appl. Surf. Sci. 203-204, 377 (2003).
[14] N. Yanagida, K. Ishibashi, S. Uchiumi and T. Inada, Nucl. Instr. and Meth. B257, 203 (2007).